Active-Matrix Driven Flexible Pressure Sensor Array Using Oxide Thin-Film Diode

Hye-In Yeom, Jingyu Kim, Guk-Jin Jeon, Joohyeong Kim, and Sang-Hee Ko Park

***Abstract*— Active-matrix (AM) flexible pressure sensor is more advantageous than a passive-matrix in terms of power consumption, contrast, and crosstalk problems. Particularly, the AM platform is frequently adopted in wearable electronic systems for accurate data processing because it offers real-time interaction between humans and the external environment. Based on the above, we reported that AM driven flexible pressure sensor array integrated with an oxide thin-film diode and AgNW-coated microstructured polydimethylsiloxane sheet. The pressure sensor exhibited a high sensitivity of 0.6 Pa^{-1} at a low-pressure regime (<1 kPa) and a short response time of 70 ms, as well as excellent electrical uniformity and mechanical durability. Additionally, upon applying the AM operation, the pressure sensor array accurately identified the selected cell to which the pressure was applied without any sneak current, unlike the passive matrix operation. Consequently, the proposed AM driven flexible pressure sensor shows promising applicability as a building block for advanced wearable platforms.**

***Index Terms*— Active-matrix, contact-type structure, flexible pressure sensor, oxide thin-film diode.**

I. Introduction

PRESSURE sensor arrays for large-area sensing are critical for wearable platforms [1], [2], [3]. These sensor arrays can sense the pressure applied to cells by sequentially applying a voltage to the longitudinal (X) line and lateral (Y) line. The driving method for the array is divided into passive-matrix (PM) and active-matrix (AM). In the case of using the PM method, due to the lack of rectifying characteristics, the current can flow even in cells where no pressure is applied, which results in inaccurate measurements [4]. The AM method, which combines switching devices and sensor arrays, allows current to flow only to cells where pressure is applied, indicating reduced signal crosstalk [5]. Further, the AM method provides improved sensing contrast, signal amplification, and low power consumption [6], [7]. Despite the complexity of the fabrication process, several studies on the AM pressure sensor array that adopt transistors have been performed [8], [9], [10].

Meanwhile, the diode used for the switching device has a simple fabrication process compared to the transistor, and can thus be applied to AM pressure sensors. There are two types of AM pressure sensor arrays that use diodes for integration with resistive pressure sensors: sandwich structures and contact-type structures with contact resistive sensors [11], [12], [13]. In the sandwich structure, piezoresistive sensing material is sandwiched between the top and bottom electrodes, wherein the bottom electrode is connected to the anode of the diode. When pressure is applied, the resistance of the sensing material decreases, thereby increasing the potential of the anode. This sandwich structure utilizes piezoresistive pressure sensors, including a wide selection of materials and a broad sensing range. However, forming the top electrode on the elastomeric materials with the bottom backplane in precise alignment remains challenging. The contact-type structure utilizes contact-resistive sensing materials and electrodes, wherein all the electrodes are on the same plane positioned under the sensor. Because the surface of the sensor is typically structured, the contact area between the electrodes and sensors increases under external pressure, leading to a decrease in contact resistance [14], [15]. Thus, a contact resistive sensor is simply loaded on the backplane after all the fabrication processes of the backplanes are completed.

In this study, we developed an AM driven flexible pressure sensor array that combines an oxide thin-film diode and AgNW-coated micropyramid (AMP) polydimethylsiloxane (PDMS) sheet with a contact-type structure. The integrated sensor showed a high sensitivity of 0.6 Pa^{-1} at a low-pressure regime of up to 1 kPa. Moreover, through real-time sensing, it was confirmed that the integrated sensor can accurately detect and discriminate the pressure without any crosstalk.

II. Experiment

The structure and fabrication process of the oxide-thin film diode are shown in Fig. 1(a). The diode array (5 × 5) was fabricated on polyimide-coated glass. Si_3N_4 (170 nm) and Al_2O_3 (30 nm) were deposited as buffer layers. ITO film (150 nm) was deposited and patterned as the cathode. Sequentially, InO_x(3 nm), Al_2O_3(20 nm), and Mo (80 nm) were deposited and patterned as active, insulators, and anode, respectively. Then, SiO_2 (500 nm) was deposited as a spacer. Mo (200 nm) was deposited, followed by patterning as the X line. Then, second spacer layers were deposited, which were constructed of three layers: Al_2O_3(30 nm), SiO_2 (500 nm),

Manuscript received 16 January 2023; revised 25 February 2023 and 11 March 2023; accepted 20 March 2023. Date of publication 23 March 2023; date of current version 26 April 2023. This work was supported in part by the Technology Development Program funded by the Ministry of SMEs and Startups (MSS), South Korea, under Grant S3207541. The review of this letter was arranged by Editor I. Nistor. *(Hye-In Yeom and Jingyu Kim contributed equally to this work.) (Corresponding author: Sang-Hee Ko Park.)*

The authors are with the Department of Materials Science and Engineering, Korea Advanced Institute of Science and Technology, Daejeon 34141, South Korea (e-mail: shkp@kaist.ac.kr).

Color versions of one or more figures in this letter are available at https://doi.org/10.1109/LED.2023.3261065.

Digital Object Identifier 10.1109/LED.2023.3261065

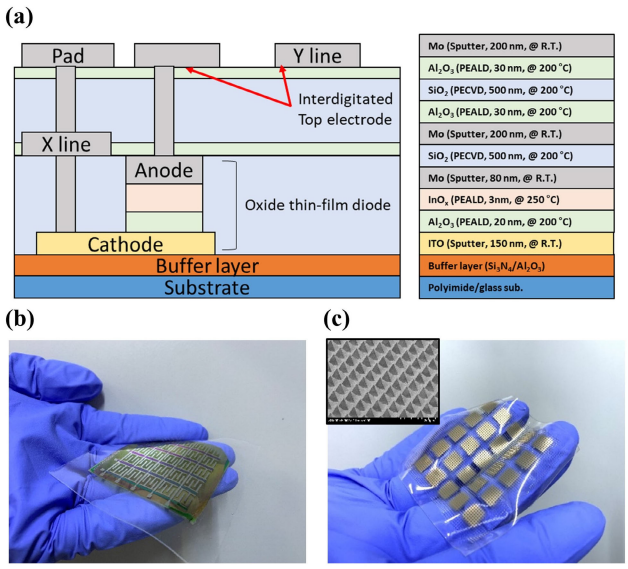

Fig. 1. (a) Structure and fabrication process of the oxide thin-film diode. (b) Optical images of the oxide thin-film diode array and (c) AMP PDMS sheet (Inset: SEM image of AMP PDMS sheet).

and Al_2O_3 (30 nm). Mo (200 nm) was deposited, followed by patterning as the Y line and interdigitated electrode for sensor contact. The electrical mechanism of the oxide thin-film diode is described in the previous paper [16]. To ensure flexibility, the device was delaminated using a laser lift-off and transferred to a PDMS substrate. An optical image of the array is shown in Fig. 1(b).

For the AMP PDMS sheet, the base and curing agent (weight ratio of 10:1) were mixed to prepare the PDMS solution (Sylgard 184, Dow Corning). Then, the prepared PDMS solution was degassed in vacuum chamber to remove air pores. Further, the PDMS solution was spin-coated on the micropyramid Si mold at 500 rpm for 30 s. The annealed condition was 80 °C for 2 h. The cured PDMS sheet was mechanically peeled off from the silicon mold, followed by O_2 plasma treatment. Furthermore, an AgNWs solution was spray-coated onto the microstructured PDMS sheet using the mask. This was carried out on 80 °C hot plate to evaporate the solvent. The optical and SEM (Nova230) images of the AMP PDMS sheet are shown in Fig. 1(c).

The electrical properties of the diode and pressure sensor array were measured by using an HP4156A semiconductor parameter analyzer. The pressure applied to the device was analyzed using a force gauge (M5-2; Mark-10). The resistance change of the pressure sensor was monitored using a digital multimeter (Keysight 34461A).

III. Results and Discussion

The 25 diode cells in the array exhibited outstanding uniformity, as shown in Fig. 2(a). The average values of the off-current, on-current, and turn-on voltage were 5.03×10^{-8} A/cm^2, 1.33×10^{-1} A/cm^2, and -0.047 V, respectively. Fig. 2(b) shows the J–V curves of the diode when pressures were applied to the device. In this range (0 to 50 kPa), the diode maintained its electrical properties regardless of the pressure. Additionally, a pressure durability test was performed by applying 50 kPa to the device 5,000 times, and the device showed no degradation, as shown in

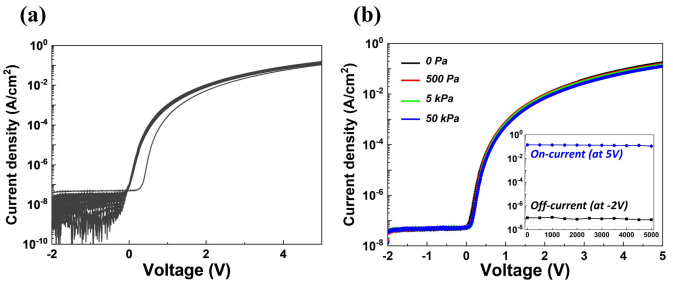

Fig. 2. (a) J–V characteristics of 25 oxide thin-film diodes in the array. (b) Pressure durability of the oxide thin-film diode (Inset: Durability of the oxide thin-film diode against cyclic pressure of 50 kPa).

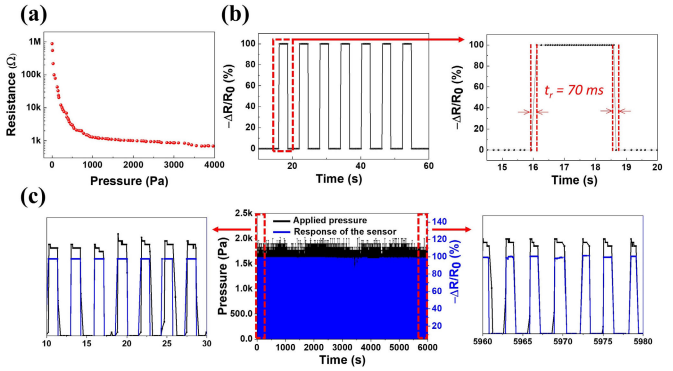

Fig. 3. (a) Change in relative resistance of the AMP PDMS sheet against pressure. (b) Relative resistance change response to successive pressure change under 1 kPa. (c) Cyclic response of the AMP PDMS sheet for 6,000 cycles under pressure of 1 kPa.

the inset of Fig. 2(b). Hence, the diode was suitable for the flexible pressure sensor array.

Fig. 3(a) shows the sensing characteristics of the AMP PDMS sheet on interdigitated electrodes with a similar size as the diode array. The resistance drastically decreased under 1 kPa and saturated at approximately 3 kPa, implying that the AMP PDMS sheet can detect targets subtle to low pressure. Fig. 3(b) shows the response time of the AMP PDMS sheet while applying and relaxing the constant pressure. When the sheet was unloaded, the relative resistance change was almost maintained. When the sheet was loaded with a pressure of 1 kPa, the relative resistance change increased rapidly, and the increased value remained almost constant. Both the rising and falling response times were approximately 70 ms. Also, the mechanical durability of the AMP PDMS sheet under 1 kPa was shown in Fig. 3(c). The results in the initial and final cycles remained almost similar with no remarkable degradation.

For the integration to configure a flexible pressure sensor array, the edges of the diode array and AMP PDMS sheet were attached using the PDMS solution, as shown in Fig. 4(a). In the case of a circuit composed of a diode and a resistor, the operating point can be analyzed through the characteristic curve of the diode and the load line which represents the linear part of the circuit. From the intersection point where the characteristic curve of the diode and load line met, it was possible to determine the amount of current flow at each pressure, as shown in Fig. 4(b). There were 4 points of intersection under the pressure from 0 to 1,000 Pa. As the sensor resistance decreased with the applied pressure, the anode voltage increased, which led to more current. Fig. 4(c)

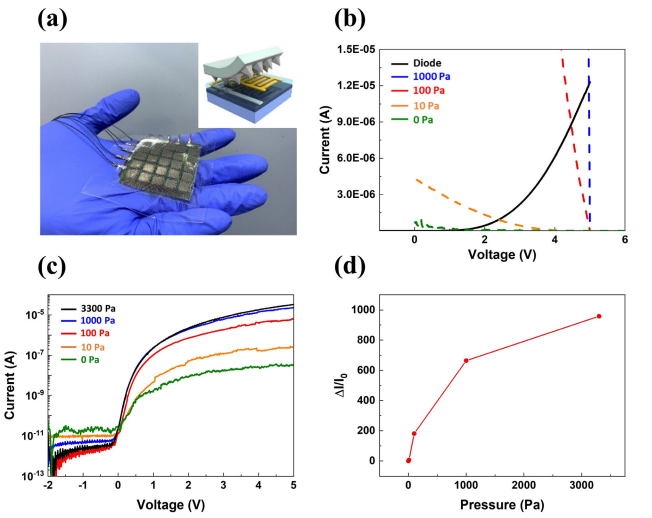

Fig. 4. (a) Optical image of flexible pressure sensor array after integration. (b) Characteristic curve of diode and load line graphs of AMP PDMS sheet against pressure. (c) I–V curves of representative cell with varying pressure. (d) Relative change in on-current (at a voltage of 5 V) with pressure. I_0 is the diode current at zero pressure.

TABLE I
COMPARISON OF THE PERFORMANCE OF PREVIOUSLY FLEXIBLE RESISTIVEPRESSURE SENSORS

Material	Sensitivity	Pressure range
Carbon composite [17]	0.3 kPa^{-1} up to 0.7 kPa	0~5 kPa
Graphene-PI foam [18]	0.36 kPa^{-1} up to ~2 kPa	0~5 kPa
PANI/BC/CH aerogels [19]	1.41 kPa^{-1} up to ~0.25 kPa	0.032~2.5 kPa
Our work	0.6 Pa^{-1} up to 1 kPa	0~3.3 kPa

shows the pressure response of a representative cell in the array. As more pressure was applied, the on-current (at a voltage of 5 V) increased until 3.3 kPa, known as the saturation pressure. The on-currents under each pressure matched the intersect points in Fig. 4(b). With these on-current values, the relationship between the relative current change and pressure was obtained, as shown in Fig. 4(d). The result exhibits a higher sensitivity of 0.60 Pa^{-1} at a low-pressure regime ($P < 1$ kPa) and lower sensitivity of 0.15 Pa^{-1} at a high-pressure regime (1 kPa $< P <$ 3.3 kPa). The performances of previously reported flexible resistive pressure sensors are summarized in Table I [17], [18], [19]. Compared with other pressure sensors, our sensor shows an extremely high sensitivity and a prominent pressure range.

The real-time data from the pressure sensor array was acquired by using the serial connection of the sensor and microcontroller unit (MCU) integrated circuit. First, a voltage (5 V) from the digital port was applied to the selected cell. When the pressure was applied to the selected cell, the current flowed as the potential of the diode anode increased. This current flowed through the reference resistor and was applied to the analog port of the Arduino board with output voltage. The voltage/current changes were calculated in the MCU and transmitted to the computer to visually express the signals from each cell.

The real-time pressure sensing performance of the PM and AM pressure sensor arrays are demonstrated in Figs. 5(a) and (b), respectively. It is clearly shown that the

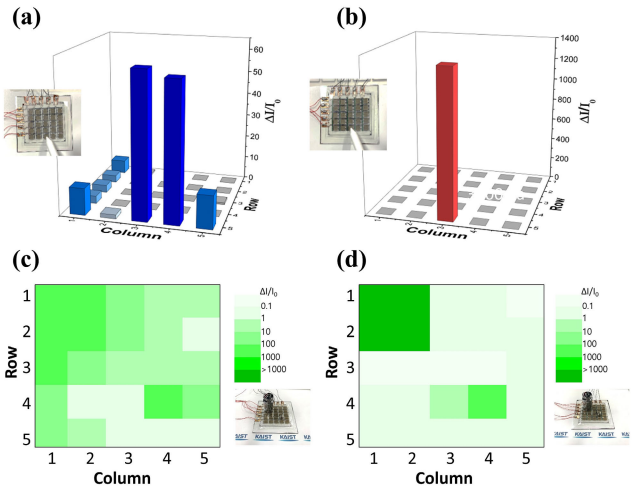

Fig. 5. The real-time sensing performance of (a) PM and (b) AM pressure sensor array. The sensing performance of (c) PM and (d) AM pressure sensor array for the detection of two spatial pressure distributions.

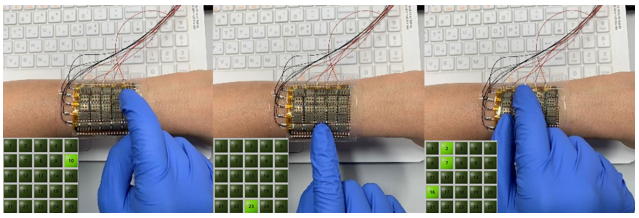

Fig. 6. The real-time sensing performance of AM pressure sensor array on human skin.

sneak current arises in the PM sensor array while the AM sensor array shows accurate sensing. For the PM sensor array, current flowed into the adjacent-pressed cells under no pressure. Here, the current flowed through the least resistive path, such as non-selected metal lines, thereby resulting in a sneak current. Contrarily, diodes in the AM sensor array blocked the sneak current owing to their rectifying capability. These phenomena were also observed in the multi-sensing performances (Figs. 5(c) and (d)). The AM pressure sensor array accurately determined the spatial distribution of both weights (1 and 50 g) as opposed to the PM pressure sensor array. In addition, the AM pressure sensor array showed excellent sensing performance even on curved human skin, as shown in Fig. 6. These results indicate that the AM pressure sensor array not only distinguishes each pressure but also accurately senses it without any crosstalk problem even under external pressure and lateral strain.

IV. CONCLUSION

We developed an AM driven flexible pressure sensor array integrated with an oxide thin-film diode and AMP PDMS sheet. The array fabrication process was simplified by using diodes instead of transistors as switching devices. The oxide thin-film diode and AMP PDMS sheet exhibited an excellent uniformity of their electrical characteristics and mechanical durability. The integrated sensor exhibited an extremely high sensitivity (0.6 Pa^{-1}) at a low-pressure regime. Further, contrary to the PM method, the pressure sensor array accurately sensed the pressure without any crosstalk by using the AM method. We believe that the proposed pressure sensor in this study is suitable for a flexible pressure sensor system that requires an array, such as e-skin.

REFERENCES

[1] Y. Duan, S. He, J. Wu, B. Su, and Y. Wang, "Recent progress in flexible pressure sensor arrays," *Nanomaterials*, vol. 12, no. 14, p. 2495, Jul. 2022.

[2] S. Ji, J. Jang, J. C. Hwang, Y. Lee, J. Lee, and J. Park, "Amorphous oxide semiconductor transistors with air dielectrics for transparent and wearable pressure sensor arrays," *Adv. Mater. Technol.*, vol. 5, no. 2, Feb. 2020, Art. no. 1900928.

[3] B. Nie, R. Huang, T. Yao, Y. Zhang, Y. Miao, C. Liu, J. Liu, and X. Chen, "Textile-based wireless pressure sensor array for human-interactive sensing," *Adv. Funct. Mater.*, vol. 29, no. 22, May 2019, Art. no. 1808786.

[4] Y. Li, J. Long, Y. Chen, Y. Huang, and N. Zhao, "Crosstalk-free, high-resolution pressure sensor arrays enabled by high-throughput laser manufacturing," *Adv. Mater.*, vol. 34, no. 21, May 2022, Art. no. 2200517.

[5] Q. Hua, H. Wu, B. Gao, M. Zhao, Y. Li, X. Li, X. Hou, M. Chang, P. Zhou, and H. Qian, "A threshold switching selector based on highly ordered Ag nanodots for X-point memory applications," *Adv. Sci.*, vol. 6, no. 10, May 2019, Art. no. 1900024.

[6] Z. Huo, Y. Peng, Y. Zhang, G. Gao, B. Wan, W. Wu, Z. Yang, X. Wang, and C. Pan, "Recent advances in large-scale tactile sensor arrays based on a transistor matrix," *Adv. Mater. Interfaces*, vol. 5, no. 21, Nov. 2018, Art. no. 1801061.

[7] J. Wang, J. Jiang, C. Zhang, M. Sun, S. Han, R. Zhang, N. Liang, D. Sun, and H. Liu, "Energy-efficient, fully flexible, high-performance tactile sensor based on piezotronic effect: Piezoelectric signal amplified with organic field-effect transistors," *Nano Energy*, vol. 76, p. 105050, Oct. 2020.

[8] C. Xin et al., "Highly sensitive flexible pressure sensor by the integration of microstructured PDMS film with a-IGZO TFTs," *IEEE Electron Device Lett.*, vol. 39, no. 7, pp. 1073–1076, Jul. 2018.

[9] S.-H. Shin, S. Ji, S. Choi, K.-H. Pyo, B. W. An, J. Park, J. Kim, J.-Y. Kim, K.-S. Li, J. Heo, B.-G. Park, and J.-U. Park, "Integrated arrays of air-dielectric graphene transistors as transparent active-matrix pressure sensors for wide pressure ranges," *Nature Commun.*, vol. 8, no. 1, pp. 1–8, 2017.

[10] T. Someya, T. Sekitani, S. Iba, Y. Kato, H. Kawaguchi, and T. Sakurai, "A large-area, flexible pressure sensor matrix with organic field-effect transistors for artificial skin applications," *Proc. Nat. Acad. Sci. USA*, vol. 101, no. 27, pp. 9966–9970, Jul. 2004.

[11] D. Geng, S. Han, H. Seo, M. Mativenga, and J. Jang, "Piezoelectric pressure sensing device using top-gate effect of dual-gate a-IGZO TFT," *IEEE Sensors J.*, vol. 17, no. 3, pp. 585–586, Feb. 2017.

[12] C. L. Choong, M. Shim, B. Lee, S. Jeon, D. Ko, T. Kang, J. Bae, S. H. Lee, K. Byun, J. Im, Y. J. Jeong, and C. E. Park, "Highly stretchable resistive pressure sensors using a conductive elastomeric composite on a micropyramid array," *Adv. Mater.*, vol. 26, no. 21, pp. 3451–3458, 2014.

[13] J. Park, Y. Lee, J. Hong, M. Ha, Y. Jung, H. Lim, S. Y. Kim, and H. Ko, "Giant tunneling piezoresistance of composite elastomers with interlocked microdome arrays for ultrasensitive and multimodal electronic skins," *ACS Nano*, vol. 8, no. 5, pp. 4689–4697, 2014.

[14] J. Shi, L. Wang, Z. Dai, L. Zhao, M. Du, H. Li, and Y. Fang, "Multiscale hierarchical design of a flexible piezoresistive pressure sensor with high sensitivity and wide linearity range," *Small*, vol. 14, no. 27, Jul. 2018, Art. no. 1800819.

[15] S. C. Mannsfeld, B. C. Tee, R. M. Stoltenberg, C. V. H. Chen, S. Barman, B. V. O. Muir, A. N. Sokolov, C. Reese, and Z. Bao, "Highly sensitive flexible pressure sensors with microstructured rubber dielectric layers," *Nature Mater.*, vol. 9, pp. 859–864, Sep. 2010.

[16] H.-I. Yeom, J. Kim, G.-J. Jeon, J. Park, D. U. Han, J. Kim, K. M. Kim, B. Shong, and S.-H.-K. Park, "High-performance oxide thin-film diode and its conduction mechanism based on ALD-assisted interface engineering," *J. Mater. Chem. C*, vol. 11, no. 4, pp. 1336–1345, Jan. 2023.

[17] K.-H. Kim, S. K. Hong, N.-S. Jang, S.-H. Ha, H. W. Lee, and J.-M. Kim, "Wearable resistive pressure sensor based on highly flexible carbon composite conductors with irregular surface morphology," *ACS Appl. Mater. Interfaces*, vol. 9, no. 20, pp. 17499–17507, May 2017.

[18] J. Yang, Y. Ye, X. Li, X. Lü, and R. Chen, "Flexible, conductive, and highly pressure-sensitive graphene-polyimide foam for pressure sensor application," *Composites Sci. Technol.*, vol. 164, pp. 187–194, Aug. 2018.

[19] J. Huang, D. Li, M. Zhao, H. Ke, A. Mensah, P. Lv, X. Tian, and Q. Wei, "Flexible electrically conductive biomass-based aerogels for piezoresistive pressure/strain sensors," *Chem. Eng. J.*, vol. 373, pp. 1357–1366, Oct. 2019.